Hindawi
International Journal of Photoenergy
Volume 2020, Article ID 3872529, 13 pages
https://doi.org/10.1155/2020/3872529

Research Article

High-Performance Standalone Photovoltaic Water Pumping System Using Induction Motor

Mustapha Errouha,[1] **Aziz Derouich**,[1] **Najib El Ouanjli**,[1] **and Saad Motahhir**[2]

[1]*Laboratory of Production Engineering, Energy and Sustainable Development, Higher School of Technology, Sidi Mohamed Ben Abdellah University, Fez, Morocco*
[2]*ENSA, SMBA University, Fez, Morocco*

Correspondence should be addressed to Mustapha Errouha; mustapha.errouha@usmba.ac.ma

Received 3 February 2020; Revised 5 June 2020; Accepted 20 July 2020; Published 18 August 2020

Academic Editor: Francesco Riganti-Fulginei

This work is aimed at achieving a simple and reduced-cost configuration of photovoltaic (PV) water pumping system (PVWPS) using an induction motor with high efficiency. The proposed PV system is composed of two stages of converters which the first one ensures the maximum power point by controlling the duty ratio of boost converter using variable step size incremental conductance (VSS INC) technique. Fuzzy logic control based on direct torque control is proposed to serve the purpose of operating an induction motor. Moreover, the combining of these proposed control strategies has been never discussed. The proposed control scheme is modeled and simulated in detail under MATLAB/Simulink software to evaluate its performance under fast variations of irradiance and daily climatic profile. The obtained simulation results using the suggested control strategies are compared to those using the most used method in the literature (variable step size perturb and observe (VSS P&O) algorithm). The simulation results indicate that the proposed PVWPS performed best in terms of the time of response; pumped water, flux ripples, and the stator currents are reduced.

1. Introduction

With the increasing use of electricity and cost diesel, finding a promising alternative to power a pumping system is required. Water pumping systems based on photovoltaic technology are good solutions for rural areas where the connection to the grid power can be difficult and expensive [1, 2]. Thus, these systems are more reliable than those based on diesel pumps, because they require less maintenance [3].

However, the performance of a PV generation system is influenced by three factors which are irradiation, nature of load, and atmospheric temperature [4]. To surmount these drawbacks, maximum power point tracking (MPPT) techniques are used to maximize the PV output power whatever the weather and operating conditions [5]. Various MPPT techniques have been reported in the literature; each method has its specification, limitation, and application. The MPPT algorithms can be classified into three major groups [6]: (i) conventional methods including constant voltage controller (CVC) method, perturb and observe (P&O) method, incremental conductance (IC) method; these kinds of algorithms use PV current, PV voltage, irradiance, and temperature for maximum power extraction and they are characterized by its simple implementation; (ii) artificial intelligence-based methods including fuzzy logic controller technique, artificial neural network control strategy, and adaptive neurofuzzy inference method. These algorithms have fast response and good MPP tracking accuracy and offer better performance than the conventional methods but they are complex to implement; (iii) hybrid methods including modified perturb and observe method (modified P&O), PI-modified fuzzy logic controller (PI-FLC) method, and neural-fuzzy logic (N-FL) method; these algorithms combine the conventional and artificial intelligence-based methods to achieve greater efficiency and tracking accuracy.

Artificial intelligent-based methods and the incremental conductance algorithm are the most recommended control strategies for PV water pumping systems [7]. Artificial

intelligent-based methods are complex and need a high-speed processor for implementation [4].

Different types of motors are used with PV-based water pumping system to drive the pump [8, 9]; the choice depends on the efficiency, the availability, the price, and the reliability. PV pumping systems based on AC motors, particularly induction motors (IM), are more attractive because these types of engines are rugged; they have high efficiency, maintenance-free, and low cost [10, 11]. Field oriented control (FOC) and direct torque control (DTC) are the most used control strategies for induction motor drives [12]. FOC assures a decoupling between the flux and torque of the motor [8, 13]; this decoupling provides very fast torque response and large speed control range. However, this technique is sensitive to the parametric variations of the motor, particularly that of the resistances whose value changes with temperature [14]. DTC technique was proposed by Takahashi to overcome some of the difficulties encountered with FOC [15, 16]. It offers remarkable dynamic performance as well as good robustness to parameter variations. However, two major disadvantages arise: (i) the ripples' amplitude of the torque and stator flux especially at low speed and (ii) the switching frequency is highly variable [17]. The torque ripples cause additional noise and mechanical vibrations. Different solutions are proposed in the literature to overcome these disadvantages [18, 19]. In this paper, a fuzzy logic controller (FLC) is proposed to improve the performance of DTC. The use of FLC allows fixing the switching frequency. Therefore, the flux ripples and THD currents are minimized.

In PV pumping systems, an IM shows good performance as compared to other commercial motors because of its greater robustness, lower cost, higher efficiency, lower maintenance cost, and availability in local markets [20]. In addition to the power exchange from PV to the IM, a DC-DC boost converter is introduced. For good utilization of PV panels, it is necessary to extract maximum power from the PV panels. For this reason, variable step size incremental conductance-based maximum power point tracking control is implemented due to its performance. On the other side, VSS INC can be implemented using the low-cost ATMega328 microcontroller in the Arduino Uno board to propose a low-cost PV system [21]. Also, the proposed PV system operates without a battery. Consequently, not only the initial cost is low but also repairing, maintenance, and replacement cost can be saved.

Several configurations of PV water pumping system have been proposed in literature. In [20], an incremental conductance- (INC-) based MPPT control technique is utilized to obtain the peak power from the PV array and scalar control for induction motor drive operation. However, the authors used the INC method based on fixed step size. Incremental conductance algorithm gives a good performance with higher accuracy, but it uses a fixed step; smaller step causes slower response and larger step results in higher oscillations [22, 23]. Therefore, the performance is reduced. The scalar control strategy is characterized by its simple structure, easy design, and low cost. However, this method provides poor response of torque and the speed accuracy is not good enough, particularly at the low speed [24]. In [25], authors have presented standalone photovoltaic water pumping system driven by a brushless DC (BLDC) motor. Perturb and observe and fuzzy logic control algorithms are used to get the maximum power and compared to evaluate the performance of the PV system. BLDC motor has high efficiency and reliability, but the rotor position of this engine is identified by using hall sensors which make the system complex and increase the cost [26]. In [27], an optimization based on genetic algorithms (GA) was effectuated for two MPPT algorithms which are perturb and observe and fuzzy techniques. On the other hand, the permanent magnet DC (PMDC) motor is used to drive the pump. The use of this kind of motor for water pumping is still not popular as it suffers from nonavailability of rare earth magnet and cost constraints [28]. GA is usually utilized to optimize other algorithms based on principles of biological evolution [29]. However, this technique cannot guarantee the identification of global minimum, is not recommended for optimizing excessively complex or very large problems, and requires much time to fine tune all parameters and achieve convergence [30].

In this paper, two control strategies are introduced to propose a simple and efficient PV water pumping system. The first strategy is based on a controller that consists of variable step size incremental conductance algorithm, in which the step is adjusted automatically depending on each operational condition in order to achieve satisfactory trade-off between the oscillations and dynamics, which leads to obtain better performance than that of incremental conductance based on fixed step. On the other hand, the second strategy is based on fuzzy DTC technique to control the induction motor. This type of motor provides good performance as compared to other commercial motors due to its rugged construction. Moreover, DTC allows to achieve better efficiency and performance than scalar control strategy.

Different authors have treated variable step size incremental conductance algorithm to extract the maximum power from the PV panel [22] and DTC based on the fuzzy logic controller to improve the performance of the IM separately [31, 32]. However, to the authors' best knowledge, the combining of these proposed control strategies has never been discussed. This allows us to propose a PV water pumping system based on the combining of variable step size incremental conductance technique and fuzzy DTC control for the first time in the literature.

Moreover, the proposed system is evaluated under real daily climatic conditions and sudden changes in solar radiation. A comparison with one of the most used MPPT in the literature (variable step size perturb and observe) is achieved. Hence, the main contribution of this work is the effective reduction of flux ripples and THD of the output currents and increasing the pumped water.

This work is structured as follows: the PVWPS components are modeled in Section 2. The control strategies which are VSS P&O, VSS INC, and FDTC are detailed in Section 3. The results and discussion are illustrated in Section 4. Finally, Section 5 summarizes the conclusions of the paper.

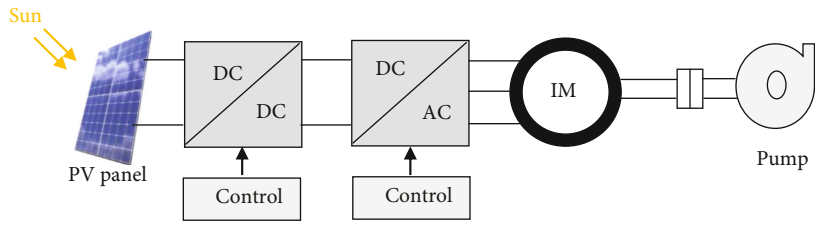

Figure 1: Synoptic diagram of the pumping system.

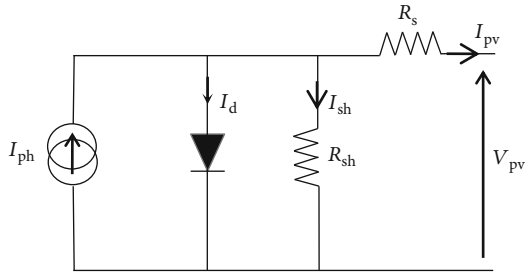

Figure 2: Equivalent circuit of a photovoltaic cell.

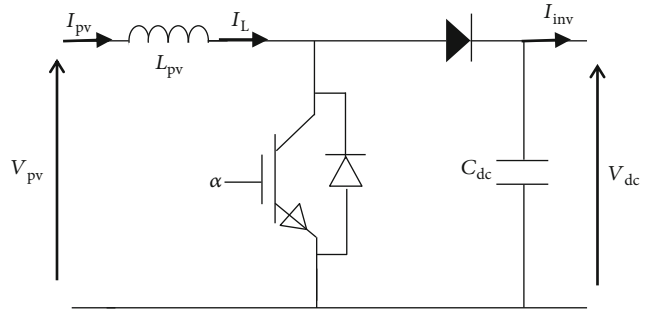

Figure 3: Boost converter.

2. Modeling of Component PV Pumping Systems

The PV pumping system (Figure 1) is composed of a PV panel, DC-DC converter controlled by MPPT algorithms, voltage source inverter (VSI) at two-level, and a centrifugal pump driven by IM.

2.1. Modeling of PV Cell. Various mathematical models explain the behavior and operation of the PV cell [33]. In this work, the single diode model is adopted (Figure 2):

From the equivalent circuit above, the output current can be calculated as follows [34, 35]:

$$I_{PV} = I_{ph} - I_O\left(\exp\frac{q(V_{PV}+R_sI)}{aKTN_s} - 1\right) - \frac{(V_{PV}+IR_s)}{R_{sh}},$$
$$I_{ph} = (I_{sc} + K_i(T - 298.15))\frac{G}{1000},$$
$$I_o = \frac{I_{sc} + K_i(T - 298.15)}{\exp((q(V_{oc}+K_v)(T - 298.15))/(aKTN_s)) - 1}. \quad (1)$$

2.2. Boost Converter. The DC-DC converter is placed between the PV panel and the inverter to increase the voltage and maximizing the power from the panel (Figure 3).

The following equation represents the mathematical model of the DC-DC converter:

$$\begin{cases} \dfrac{dV_{dc}}{dt} = \dfrac{1}{C_{dc}}\left((1-\alpha)\cdot I_{pv} - I_{inv}\right), \\ \dfrac{dI_{pv}}{dt} = \dfrac{1}{L_{pv}}\left(-(1-\alpha)\cdot V_{dc} + V_{pv}\right). \end{cases} \quad (2)$$

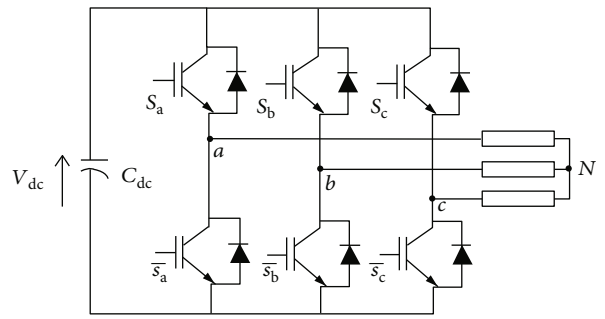

Figure 4: General structure of VSI.

2.3. Voltage Source Inverter. The voltage source inverter (VSI) model is composed of six IGBT switches and controlled by analog values [36]. The structure of VSI is illustrated in Figure 4.

Equation (3) represents the mathematical model of VSI as follows:

$$\begin{bmatrix} V_a \\ V_b \\ V_c \end{bmatrix} = \frac{V_{dc}}{3}\cdot\begin{bmatrix} 2 & -1 & -1 \\ -1 & 2 & -1 \\ -1 & -1 & 2 \end{bmatrix}\cdot\begin{bmatrix} S_a \\ S_b \\ S_c \end{bmatrix}, \quad (3)$$

where S_a, S_b, and S_c are the logic control signals and V_{dc} is the input DC voltage.

2.4. Induction Motor. The model of the IM suitable for direct torque controls which is the two-phase model (α, β) is described by the following equation:

$$\begin{cases} \dfrac{dI_{\alpha s}}{dt} = -\left(\dfrac{R_s}{\sigma l_s} - \dfrac{R_r}{\sigma l_r}\right) I_{\alpha s} - w_r I_{\beta s} + \dfrac{R_r}{\sigma l_r l_s}\psi_{\alpha s} + \dfrac{w_r}{\sigma l_s}\psi_{\beta s} + \dfrac{1}{\sigma l_s} V_{\alpha s}, \\ \dfrac{dI_{\beta s}}{dt} = -\left(\dfrac{R_s}{\sigma l_s} - \dfrac{R_r}{\sigma l_r}\right) I_{\beta s} - w_r I_{\alpha s} + \dfrac{R_r}{\sigma l_r l_s}\psi_{\beta s} - \dfrac{w_r}{\sigma l_s}\psi_{\alpha s} + \dfrac{1}{\sigma l_s} V_{\beta s}, \\ \dfrac{d\psi_{\alpha s}}{dt} = V_{\alpha s} - R_s I_{\alpha s}, \\ \dfrac{d\psi_{\beta s}}{dt} = V_{\beta s} - R_r I_{\beta s}, \end{cases} \tag{4}$$

where σ, τ_s, and τ_r are given as follows: $\sigma = 1 - (M^2/L_s L_r)$, $\tau_s = R_s/L_s$, and $\tau_r = R_r/L_r$,where $I_{\alpha s}$, $I_{\beta s}$ are the stator current components, $\psi_{\alpha s}$, $\psi_{\beta s}$ are the stator flux components, R_s, R_r are the stator and rotor resistances, l_s, l_r are the stator and rotor inductances, $M$is the mutual stator-rotor inductance, and w_r is the rotor speed.

The electromagnetic torque in the reference frame (α, β) and the movement are expressed as follows:

$$\begin{aligned} T_{em} &= \frac{3}{2} P\left(\psi_{\alpha s} i_{\beta s} - \psi_{\beta s} i_{\alpha s}\right), \\ J\frac{d\Omega}{dt} + f\Omega &= T_{em} - T_r, \end{aligned} \tag{5}$$

where p is the number of pole pairs, and f is the coefficient of friction.

2.5. Centrifugal Pump. As shown in Equation (6), the centrifugal pump load torque T_r is given as follows:

$$T_r = K \cdot \Omega^2, \tag{6}$$

where K is the pump constant.

Using the similarity laws (Equation (7)), the characteristic of the centrifugal pump can be obtained for any rotation speed [37].

$$Q' = Q \cdot \left(\frac{N'}{N}\right), \tag{7}$$

$$H' = H \cdot \left(\frac{N'}{N}\right)^2, \tag{8}$$

$$P' = P \cdot \left(\frac{N'}{N}\right)^3. \tag{9}$$

3. Control Strategies

3.1. MPPT Algorithms. In this paper, two MPPT algorithms have been chosen for comparison: variable step size perturb and observe (VSS P&O) and variable step size incremental conductance (VSS INC).

3.1.1. Variable Step Size Perturb and Observe. The P&O algorithm is used by the majority of authors because it is easy and simple to implement and is low-cost [38]. Based on the measuring of PV voltage and current, the PV power is calculated; this latter is compared with the previous power to deduce the value of the duty cycle α. The perturb and observe algorithm is functioned as follows:

(i) If $dP_{pv}/dV_{pv} \succ 0$, the working point is on the left of the MPP

(ii) If $dP_{pv}/dV_{pv} \prec 0$, the working point is on the right of the MPP

(iii) If $dP_{pv}/dV_{pv} \approx 0$, the working point is at the MPP

The conventional P&O MPPT is based on the fixed step; smaller step causes slower response and larger step results in higher oscillations. To overcome this drawback, the variable step size is used which consists to choose automatically the step. The step size is determined by Equation (10). Figure 5 shows the flowchart of the VSS P&O algorithm.

$$\text{Offset} = \text{Ofseet0} * \left(\frac{\Delta P}{\Delta V}\right). \tag{10}$$

3.1.2. Variable Step Size Incremental Conductance. The incremental conductance algorithm has been proposed which is based on the derivative of the P_{pv} with respect to V_{pv} to avoid the disadvantages of the P&O algorithm. The principal advantage of the incremental conductance (INC) algorithm is that it provides good performance under rapidly changing atmospheric conditions. This technique uses the slope of the P_{pv} characteristics to track MPP [39]. Therefore, incremental conductance algorithm is operated as follows:

(i) $V_{pv}/I_{pv} = -\Delta V_{pv}/\Delta I_{pv}$ at MPP

(ii) $V_{pv}/I_{pv} \prec -\Delta V_{pv}/\Delta I_{pv}$ left to MPP

(iii) $V_{pv}/I_{pv} \succ -\Delta V_{pv}/\Delta V_{pv}$ right to MPP

The drawback of the incremental conductance method is the use of a fixed tracking step size. For this, the variable step size incremental conductance is used in this paper. Figure 6 shows the flowchart of VSS INC algorithm.

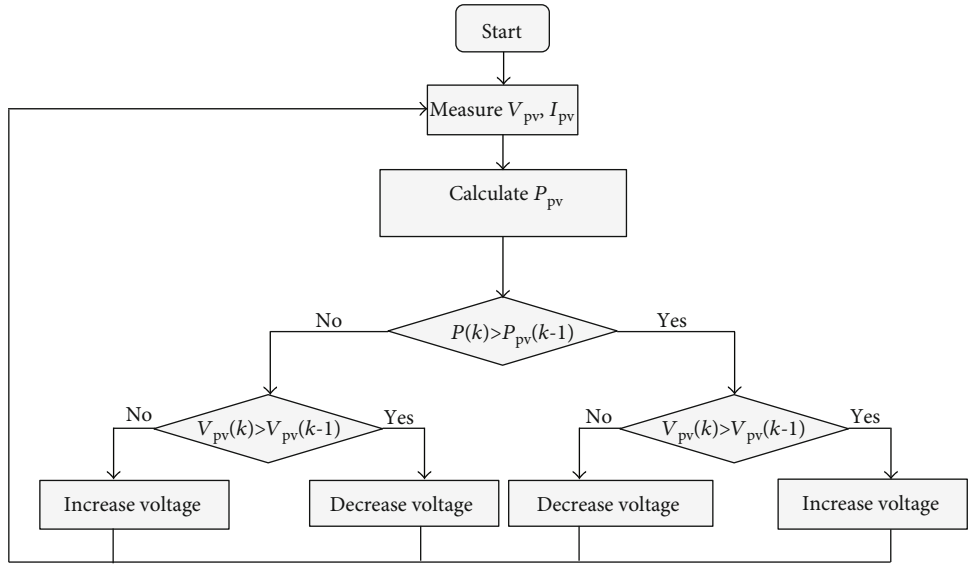

Figure 5: Variable step size P&O.

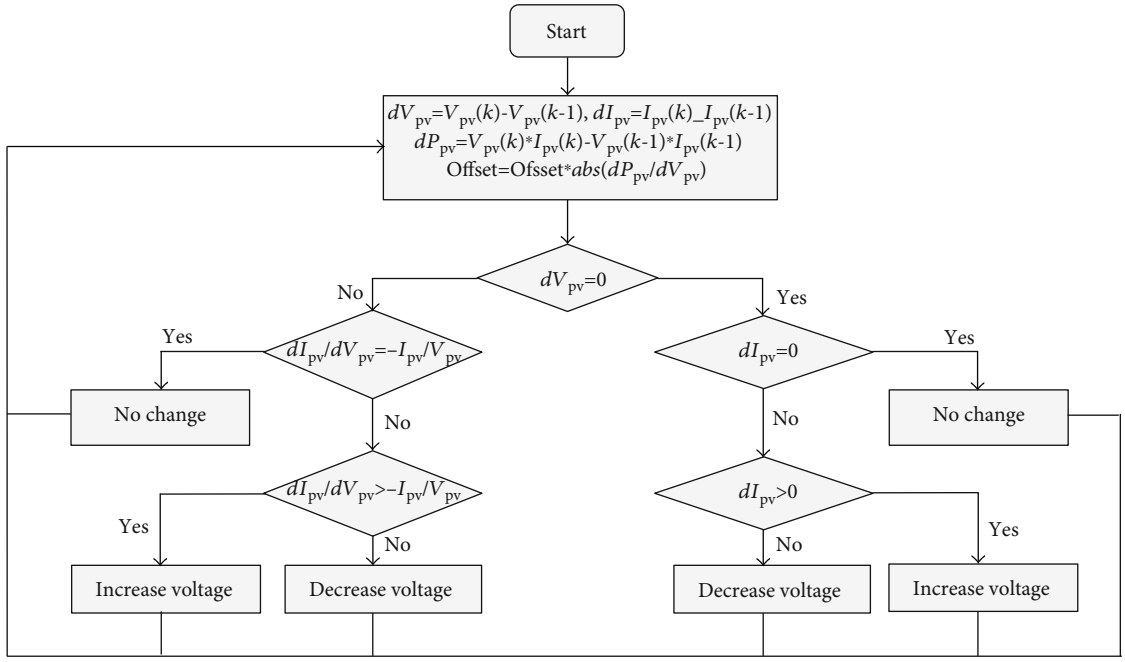

Figure 6: Variable step size incremental conductance.

3.2. Fuzzy Direct Torque Control for Induction Motor. The concept of fuzzy direct torque control (FDTC) is similar to classical DTC. It consists in regulating the flux and torque of the IM by the selection of one of the eight voltage vectors generated by each voltage inverter; this choice is made by switching the table. However, this table is elaborated by the reasoning of fuzzy logic from the flux error, torque error, and position of flux vector. This technique is characterized by good precision, stability, a good torque response, robustness, and simplicity of implementation. The principle of FDTC for the IM is shown in Figure 7.

3.2.1. Stator Flux and Torque Estimation. FDTC of the IM relies on the estimation of the magnitude to be controlled, namely, the stator flux and electromagnetic torque.

The components of stator flux can be estimated as follows:

$$\begin{cases} \widehat{\varphi}_{s\alpha} = \displaystyle\int_0^t \left(v_{s\alpha} - R_s \cdot i_{s\alpha}\right) \cdot dt, \\ \widehat{\varphi}_{s\beta} = \displaystyle\int_0^t \left(v_{s\beta} - R_s \cdot i_{s\beta}\right) \cdot dt. \end{cases} \tag{11}$$

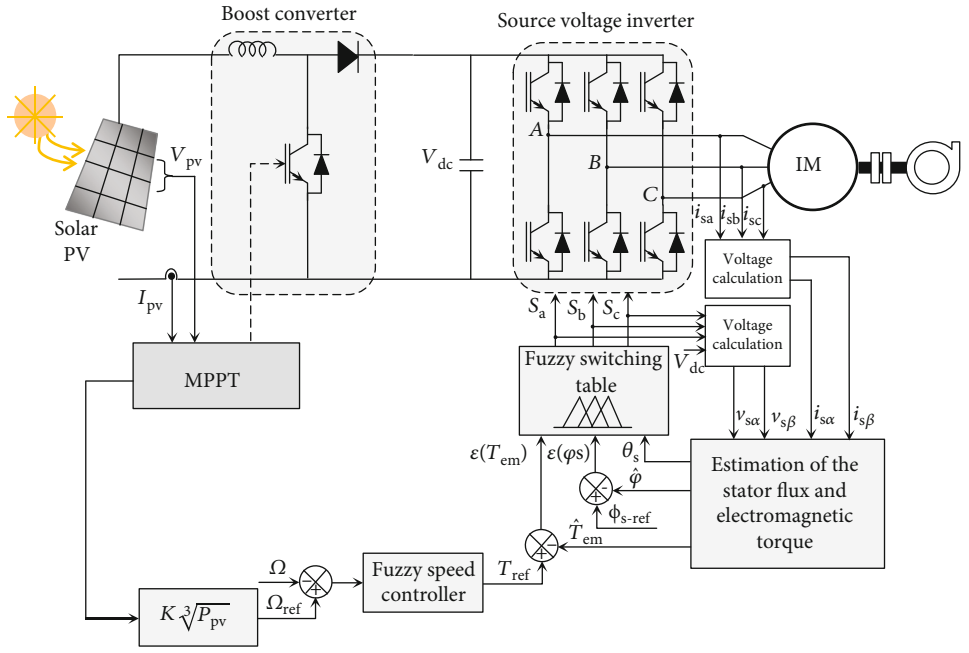

Figure 7: Synoptic scheme of FDTC for induction motor.

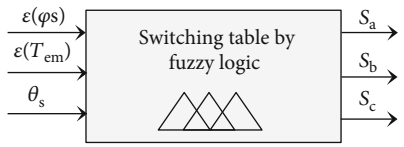

Figure 8: Fuzzy logic switching table.

The modulus and angle of the stator flux are calculated as follows:

$$\begin{aligned}\widehat{\varphi}_s &= \sqrt{\widehat{\varphi}_{s\alpha}^2 + \widehat{\varphi}_{s\beta}^2},\\ \theta_s &= \operatorname{arctg}\left(\frac{\widehat{\varphi}_{s\beta}}{\widehat{\varphi}_{s\alpha}}\right).\end{aligned} \tag{12}$$

The torque is found by the estimated flux and currents as follows:

$$T_{em} = p \cdot \left(\widehat{\varphi}_{s\alpha} \cdot i_{s\beta} - \widehat{\varphi}_{s\beta} \cdot i_{s\alpha}\right). \tag{13}$$

The currents $i_{s\alpha}$ and $i_{s\beta}$ are obtained from the measurement of the real currents i_{sa}, i_{sb}, and i_{sc}, and by the application of the transformation of Concordia, we obtain the following:

$$\begin{cases} i_{s\alpha} = \sqrt{\dfrac{2}{3}} i_{sa}, \\ i_{s\beta} = \dfrac{1}{\sqrt{2}}\left(i_{sb} - i_{sc}\right). \end{cases} \tag{14}$$

The stator voltage depends on the switches state (S_a, S_b, S_c) and the DC voltage V_{dc}; applying the Concordia transformation, we obtain the following:

$$\begin{cases} v_{s\alpha} = \sqrt{\dfrac{2}{3}} V_{dc} \cdot \left(S_a - \dfrac{1}{2}\left(S_b + S_c\right)\right), \\ v_{s\beta} = \dfrac{1}{\sqrt{2}} V_{dc}\left(S_b - S_c\right). \end{cases} \tag{15}$$

3.2.2. Fuzzy Switching Table. The switching table used in conventional DTC and the hysteresis controllers are replaced by a fuzzy switching table; the latter is built using a FLC; the inputs of this fuzzy controller are the error of the stator flux $\varepsilon_{(\varphi s)}$, electromagnetic torque error $\varepsilon_{(\mathrm{Tem})}$, and flux position θ_s (Figure 8).

Generally, the control by fuzzy logic is done in three steps: fuzzification, the establishment of rules binding the outputs to the inputs called fuzzy inference, and defuzzification.

3.2.3. Fuzzification. The purpose of fuzzification is to convert physical input variables into fuzzy variables, by defining membership functions for different input variables; the fuzzy system performance is described using a fuzzy rule base. Approximate reasoning will be done by associating the input variable with fuzzy rules using a fuzzy inference engine.

The first input of FLC is stator flux error; its universe of discourse is composed of three fuzzy variables: positive (P), zero (Z), and negative (N). The (Z) variable is represented by a triangular membership function, while (P) and (N) variables are represented by two trapezoidal membership functions (Figure 9(a)).

The torque error is composed of five fuzzy variables: positive small (PS), positive large (PL), zero (Z), negative large

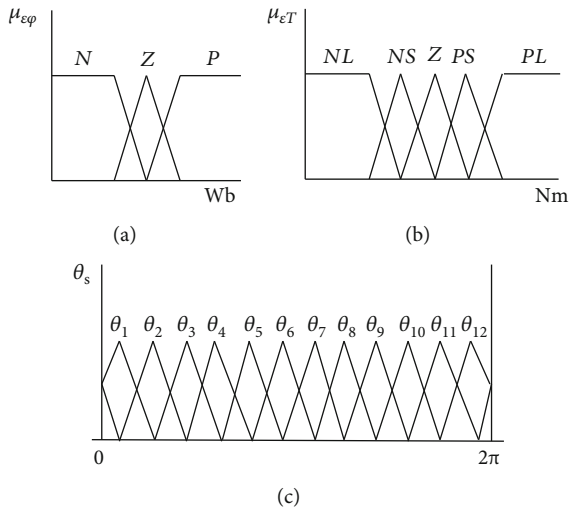

Figure 9: Membership functions of (a) flux error, (b) torque error, and (c) flux position.

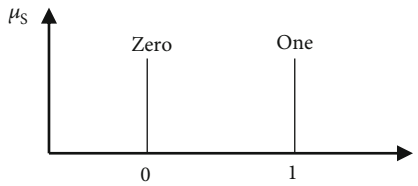

Figure 10: Membership functions of output variables.

(*NL*), and negative small (*NS*). The membership function of torque error is represented by two symmetric trapezoidal and three triangular (Figure 9(b)).

The last input of FLC is the stator flux angle; its universe of discourse is divided into 12 fuzzy sets. This input is represented by twelve membership functions triangular of 60° wide and an overlap of 30° with neighborhood fuzzy sets which each fuzzy set works for an angle of 30° (Figure 9(c)).

Figure 9 gives the membership functions for the input variables of the switching table. The output variable is illustrated in Figure 10, which is represented in our case by the switching state of the voltage inverter and defined by three output groups (S_a, S_b, S_c); the discourse universe of each output is divided into two fuzzy sets (0 and 1).

3.2.4. Fuzzy Control Rule. The optimal switching state is given by fuzzy rules, which are established using expert knowledge and intuition to govern the behavior of FLC. The control algorithm has 180 rules; the method adopted is the Max–Min inference (Mamdani method).

$$\begin{aligned} \alpha_i &= \min\left(\mu_{Ai}(\varepsilon_\varphi), \mu_{Bi}(\varepsilon_{Tem}), \mu_{Ci}(\theta)\right), \\ \mu'_{Vi}(V) &= \max\left(\alpha_i, \mu_{Vi}(V)\right), \end{aligned} \tag{16}$$

where $\mu_{Ai}(\varepsilon_\varphi)$, $\mu_{Bi}(\varepsilon_{Tem})$, and $\mu_{Ci}(\theta)$ represent the membership values of torque error, flux error, and stator flux angle and α_i is the weighting factor for its rules.

Table 1: Fuzzy control rules.

$\varepsilon_{(\varphi s)}$	$\varepsilon_{(Tem)}$	θ_1	θ_2	θ_3	θ_4	θ_5	θ_6	θ_7	θ_8	θ_9	θ_{10}	θ_{11}	θ_{12}
PL		V_2	V_3	V_3	V_4	V_4	V_5	V_5	V_6	V_6	V_1	V_1	V_2
PS		V_2	V_2	V_3	V_3	V_4	V_4	V_5	V_5	V_6	V_6	V_1	V_1
Z	*P*	V_0	V_7	V_0	V_7	V_0	V_7	V_0	V_7	V_0	V_7	V_0	V_7
NS		V_1	V_1	V_2	V_2	V_3	V_3	V_4	V_4	V_5	V_5	V_6	V_6
NL		V_6	V_1	V_1	V_2	V_2	V_3	V_3	V_4	V_4	V_5	V_5	V_6
PL		V_2	V_3	V_3	V_4	V_4	V_5	V_5	V_6	V_6	V_1	V_1	V_2
PS		V_2	V_3	V_3	V_4	V_4	V_5	V_5	V_6	V_6	V_1	V_1	V_2
Z	*Z*	V_7	V_0	V_7	V_0	V_7	V_0	V_7	V_0	V_7	V_0	V_7	V_0
NS		V_7	V_0	V_7	V_0	V_7	V_0	V_7	V_0	V_7	V_0	V_7	V_0
NL		V_6	V_1	V_1	V_2	V_2	V_3	V_3	V_4	V_4	V_5	V_5	V_6
PL		V_3	V_4	V_4	V_5	V_5	V_6	V_6	V_1	V_1	V_2	V_2	V_3
PS		V_4	V_4	V_5	V_5	V_6	V_6	V_1	V_1	V_2	V_2	V_3	V_3
Z	*N*	V_7	V_0	V_7	V_0	V_7	V_0	V_7	V_0	V_7	V_0	V_7	V_0
NS		V_5	V_5	V_6	V_6	V_1	V_1	V_2	V_2	V_3	V_3	V_4	V_4
NL		V_5	V_6	V_6	V_1	V_1	V_2	V_2	V_3	V_3	V_4	V_4	V_5

The fuzzy rules which determine the output variables of controller depending on input variables are presented in Table 1.

3.2.5. Defuzzification. This step converts the fuzzy values back into a numerical value at the output, which is one zero voltage (V_0 or V_7) and six nonzero voltage vectors. For this step, the max method is used and expressed by Equation (17). From this method, the fuzzy output value which has the maximum possibility distribution is used as a control output.

$$\mu'_{Vout}(V) = \max_{i=1}^{180} \max\left(\mu'_{Vout}(V)\right), \tag{17}$$

where μ'_{Vout} is a membership degree of the output variable.

3.3. Rotation Speed Controller by Fuzzy Logic. To overcome the troubles of classical speed controller, such as static error, sensitivity, and overshoot, we propose a FLC with as input the error and the derivation of speed error. The two fuzzy controller inputs are the speed error and its variation [40].

The speed error noted e is defined as follows:

$$e(k) = \Omega_{ref}(k) - \Omega(k). \tag{18}$$

The variation of the speed error noted Δe is defined as follows:

$$de(k) = e(k) - e(k-1). \tag{19}$$

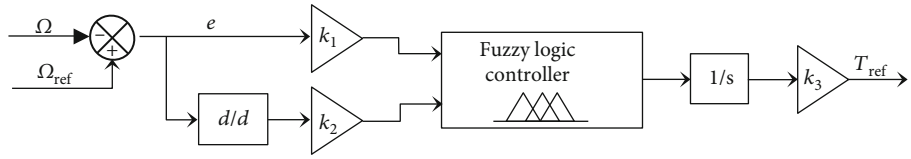

Figure 11: Structure of fuzzy logic controller.

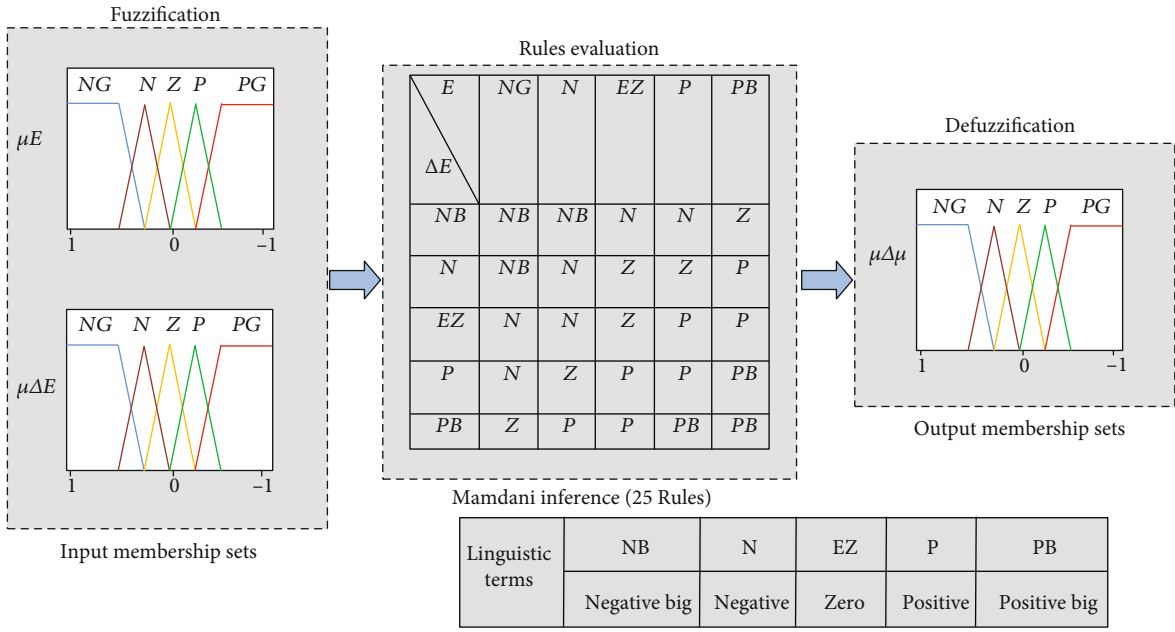

Figure 12: Internal structure of fuzzy speed controller.

Table 2: Characteristics of the Csun235-60p PV Panel.

Photovoltaic panel CSUN235-60P	
Maximum power (P_{max})	235 W
Open-circuit voltage (Voc)	36.8 V
Short-circuit current (Isc)	8.59 A
Maximum power voltage (P_{max}, Vmpp)	29.5 V
Maximum power current (P_{max}, Impp)	7.97 A
Standard test condition (STC)	1000 W/m^2, 25°C, AM 1.5
Number of cells	60
Temperature coefficient of open-circuit voltage (Voc, K_v)	-0.37%/°C
Temperature coefficient of short-circuit current (Isc, K_i)	0.07%/°C

Table 3: Parameters of Induction Motor.

Parameters	Values
Stator resistance	4.58 Ω
Rotor resistance	3.805 Ω
Stator inductance	0.274 H
Rotor inductance	0.274 H
Mutual inductance	0.258 H
Inertia moment	0.031 kg m^2
Nominal power	1.5 kW
Viscous friction	0.00114 N.m.s/rad
Pole pairs' number	2

Table 4: Design of Parameters of the System.

Component	Expression	Used value
V^*_{dc}	$V_{dc} = 2\sqrt{2}/\sqrt{3}V_{LL}$.	400 V
C_{dc}	$C_{dc} = 6\alpha V_{LL} I_t / \left[V^{*2}_{dc} - V^2_{dc1}\right]$.	2000 μF
α	$\alpha = V_{dc} - V_{mp}/V_{dc}$.	0.26
L_{pv}	$L_{pv} = DV_{mp}/\Delta I.f_s$.	3 mH

The controller output corresponds to the torque noted Δu. The three magnitudes, e, Δe, and Δu, are normalized as follows:

$$\begin{cases} E = K_1 \cdot e, \\ \Delta E = K_2 \cdot \Delta E, \\ \Delta u = K_3 \cdot \Delta u, \end{cases} \quad (20)$$

where K_1, K_2, and K_3 are scale or standardization factors and play a decisive role in the static and dynamic performance of the control.

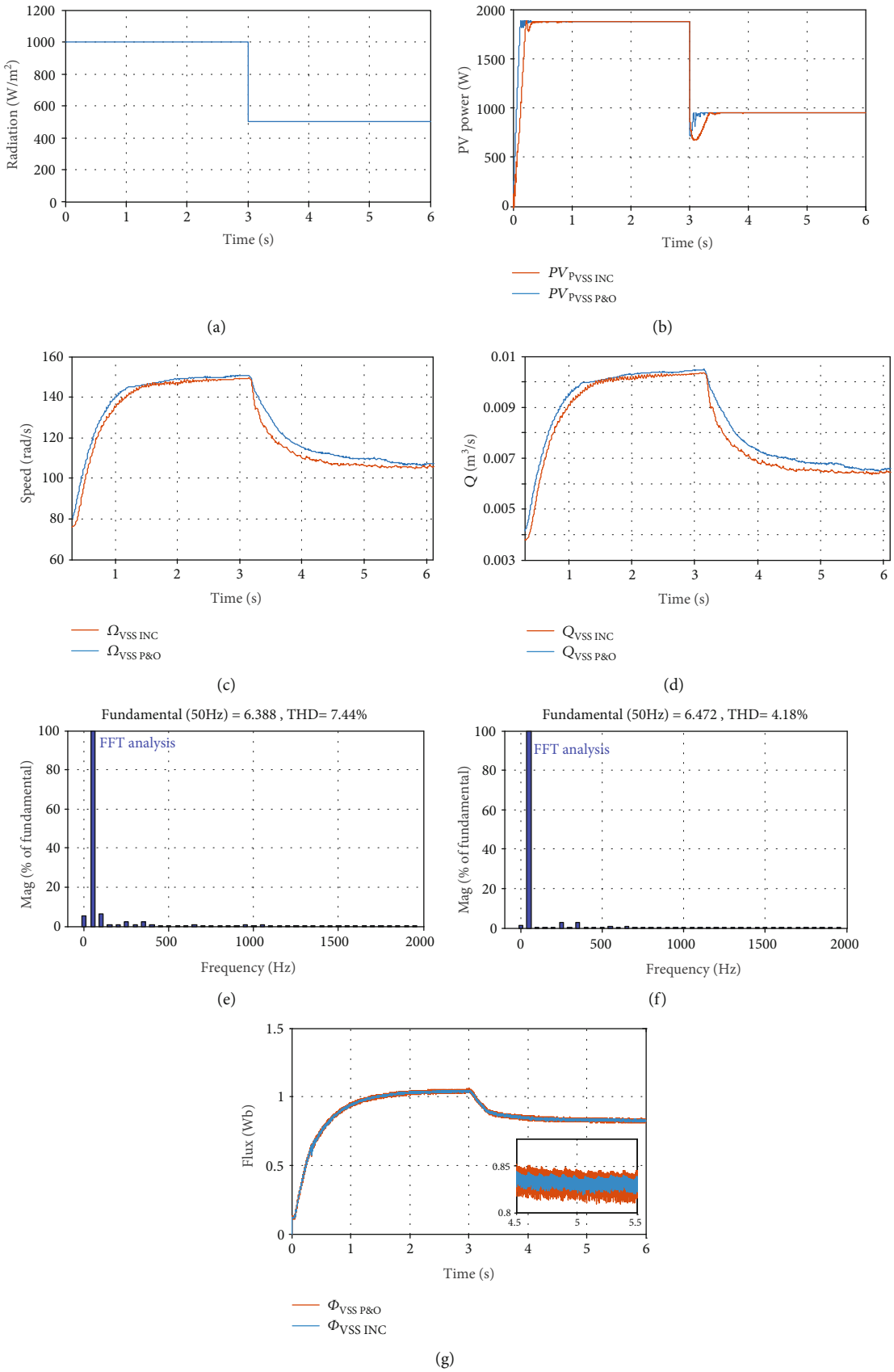

Figure 13: Results of sudden change in solar radiation: (a) irradiation profile, (b) photovoltaic power, (c) electric speed, (d) water flow, (e) FFT analysis of stator current using VSS P&O, (f) FFT analysis of stator current using VSS INC, and (g) flux response.

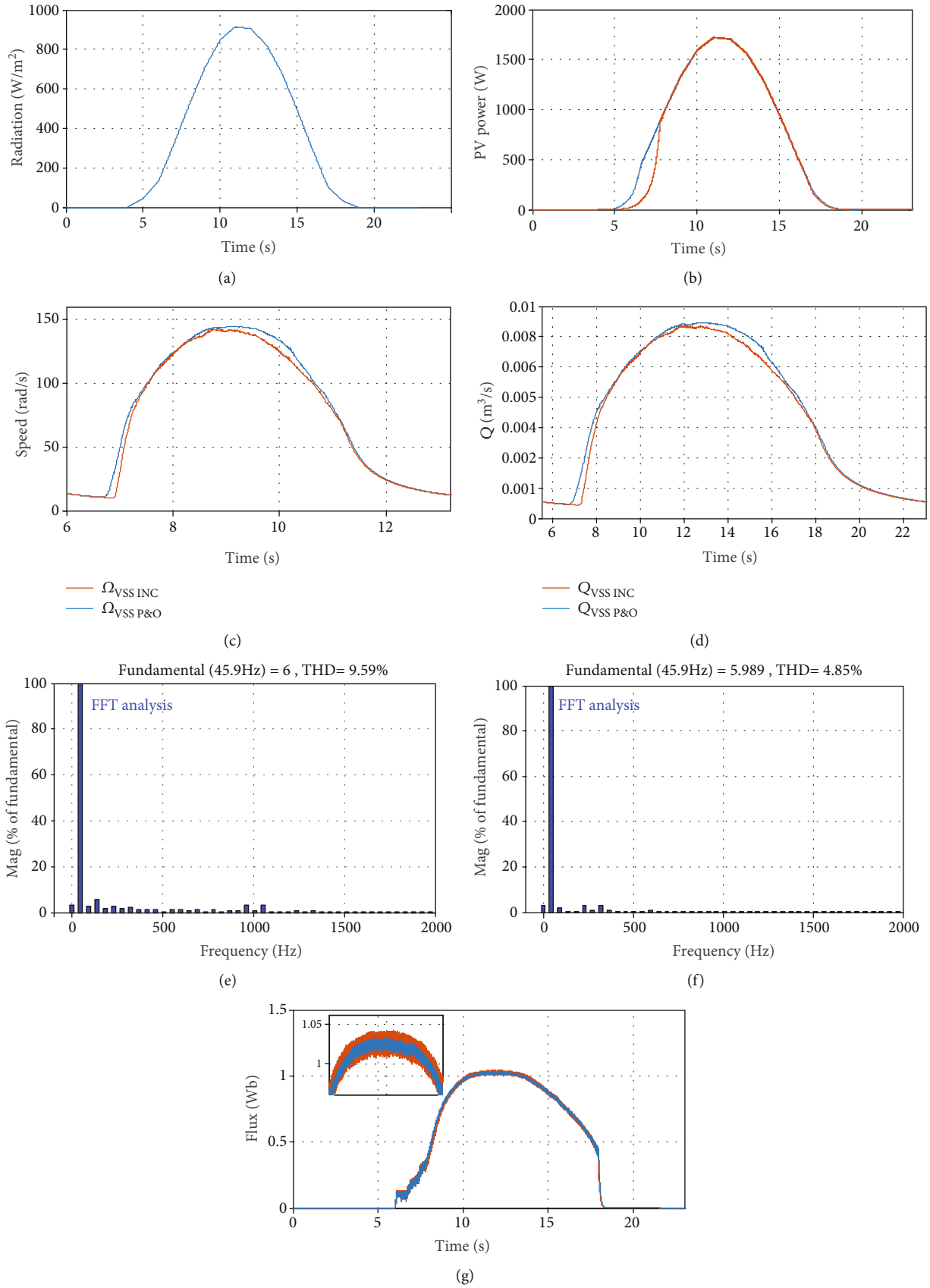

Figure 14: Results of daily profile: (a) irradiation profile, (b) photovoltaic power, (c) electric speed, (d) water flow, (e) FFT analysis of stator current using VSS P&O, (f) FFT analysis of stator current using VSS INC, and (g) flux response.

Table 5: Comparison between the proposed PVWPS and the PV system based on VSS P&O.

Irradiation (W/m^2)	Performance VSS P&O Response time	VSS P&O Ripple flux (Wb)	VSS P&O THD current (%)	Performance VSS INC Response time	VSS INC Ripple flux (Wb)	VSS INC THD current (%)	Improvements (%) Response time	Ripple flux	THD current
500	0.37 s	0.023	7.44	0.20s	0.0042	4.18	45.94	81.73	43.81
1000	0.35 s	0.029		0.25 s	0.007		28.57	75.86	
Daily profile	5.1 h	0.031	9.59	4.6 h	0.009	4.85	9.80	70.96	49.42

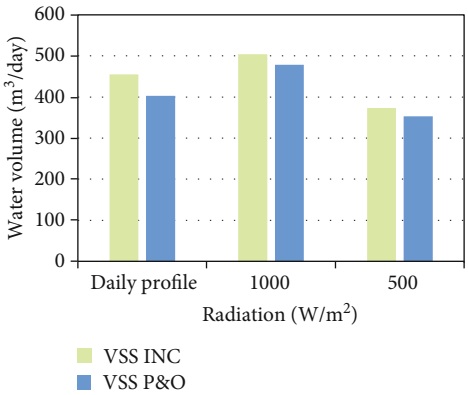

Figure 15: Water volume comparison.

Figure 11 illustrates the schema of the fuzzy speed controller. The control rules must be expressed in terms of the input and output variables using the decision table; the decision rules are described as if E is A and ΔE is B, then Δu is C. The internal structure of the fuzzy speed controller is shown in Figure 12.

4. Simulation Results

To evaluate the performance and the robustness of the studied system, different tests are carried out using MATLAB/Simulink software. Eight PV panels (CSUN 235-60P shown in Table 2) are connected in series to get power enough to run the motor of 1.5 kW (its parameters are given in Table 3). The sizing of the PVWPS components is summarized in Table 4.

4.1. Sudden Change in Solar Radiation. Solar radiation is varied from 1000 W/m^2 to 500 W/m^2 at 3 s (Figure 13(a)) to examine the dynamic and steady-state performance of the proposed PV water pumping system.

Figure 13(b) shows the response of VSS P&O and VSS INC algorithms. It can be seen that response time is reduced, and oscillations are minimized compared to VSS P&O. Figure 13(c) illustrates the evolution of electric speed using both MPPT algorithms. The simulation results show that in rapid changing in atmospheric conditions, PWPS based on VSS INC algorithm shows better response as compared to VSS P&O algorithm in terms of tracking speed.

Moreover, the pumped water volume obtained shown in Figure 13(d) is clearly higher using VSS INC. Figure 13(g) shows the developed flux responses of IM with a zoom-in view using VSS P&O and VSS INC; this latter presents low flux ripple under different values of solar radiation. To illustrate the impact of the MPPT algorithms on the quality of the signal, a FFT (fast Fourier transform) analysis of the stator current waveforms is done. Figures 13(e) and 13(f) show the frequency spectrum. It can be seen that VSS INC provides a lower total harmonic distortion (THD) in comparison with the VSS P&O.

4.2. Test under Daily Profile. In this section, a simulation test is carried out using the real data of solar radiation from Fez, Morocco for June 2016. The evolution of solar radiance is shown in Figure 14(a).

Figure 14(b) shows the PV power using the VSS P&O and VSS INC; it is clear that using this latter, the PV power increases rapidly than VSS P&O.

Figures 14(c) and 14(d) show the corresponding speed responses and the pumped water volume, respectively. The simulation results show that for a daily profile, the proposed system based on VSS INC method shows better response in terms of tracking speed and the pumped volume is clearly higher. Figures 14(e) and 14(f) show the frequency spectrum. It can be seen that the total harmonic distortion (THD) is equal to 4.85% using VSS INC. Contrary to VSS P&O method, the total harmonic distortion is equal to 9.59% that means that the quality of motor current is improved using VSS INC algorithm. Figure 14(g) shows the developed flux responses of IM. The simulation results illustrate that the response of the stator flux magnitude of VSS INC method represents low oscillations compared with VSS P&O and improved by 81.73%, 75.86%, and 70.96% under 500 W/m^2, 1000 W/m^2, and daily profile, respectively.

The system performances of both techniques are compared in terms of the response time, flux ripples, THD current, and daily pumped water and represented in Table 5. From the presented data and Figure 15, PVWPS-based VSS INC provides high performances than VSS P&O with increasing pumped water flow, maintaining a fast response time and reducing flux ripple and THD current.

5. Conclusion

In this paper, a standalone photovoltaic water pumping system without battery storage is investigated. The proposed system consists of using a variable step size incremental conductance method to adjust the duty ratio and fuzzy logic control based on DTC to control the induction motor. The innovative aspect of this paper is to propose a PV water

pumping system which combined a variable step size incremental conductance method and fuzzy logic controller based on DTC; this combination has never been discussed. The efficiency of the proposed system has been studied under different operating conditions. For more accuracy, the obtained results are compared to those using the variable step size perturb and observe method. The proposed PV water pumping system based on VSS INC presents a better performance in terms of the time of response pumped water; flux ripples and the stator currents are reduced around 4.84%.

Data Availability

The data used to support the findings of this study have not been made available because it is confidential.

Conflicts of Interest

The authors declare that they have no conflicts of interest.

References

[1] H. Drissi, J. Khediri, W. Zaafrane, and E. Ben Braiek, "Critical factors affecting the photovoltaic characteristic and comparative study between two maximum power point tracking algorithms," *International Journal of Hydrogen Energy*, vol. 42, no. 13, pp. 8689–8702, 2017.

[2] M. Matam, V. R. Barry, and A. R. Govind, "Optimized reconfigurable PV array based photovoltaic water-pumping system," *Solar Energy*, vol. 170, pp. 1063–1073, 2018.

[3] S. S. Chandel, M. N. Naik, and R. Chandel, "Review of performance studies of direct coupled photovoltaic water pumping systems and case study," *Renewable and Sustainable Energy Reviews*, vol. 76, pp. 163–175, 2017.

[4] N. Karami, N. Moubayed, and R. Outbib, "General review and classification of different MPPT techniques," *Renewable and Sustainable Energy Reviews*, vol. 68, pp. 1–18, 2017.

[5] A. Sellami, K. Kandoussi, R. El Otmani, M. Eljouad, O. Mesbahi, and A. Hajjaji, "A novel auto-scaling MPPT algorithm based on perturb and observe method for photovoltaic modules under partial shading conditions," *Applied Solar Energy*, vol. 54, no. 3, pp. 149–158, 2018.

[6] A. Gupta, Y. K. Chauhan, and R. K. Pachauri, "A comparative investigation of maximum power point tracking methods for solar PV system," *Solar Energy*, vol. 136, pp. 236–253, 2016.

[7] D. H. Muhsen, T. Khatib, and F. Nagi, "A review of photovoltaic water pumping system designing methods, control strategies and field performance," *Renewable and Sustainable Energy Reviews*, vol. 68, pp. 70–86, 2017.

[8] M. Errouha, A. Derouich, S. Motahhir, and O. Zamzoum, "Optimal control of induction motor for photovoltaic water pumping system," *Technology and Economics of Smart Grids and Sustainable Energy*, vol. 5, no. 1, 2020.

[9] C. Gopal, M. Mohanraj, P. Chandramohan, and P. Chandrasekar, "Renewable energy source water pumping systems–A literature review," *Renewable and Sustainable Energy Reviews*, vol. 25, pp. 351–370, 2013.

[10] B. Talbi, F. Krim, T. Rekioua, S. Mekhilef, A. Laib, and A. Belaout, "A high-performance control scheme for photovoltaic pumping system under sudden irradiance and load changes," *Solar Energy*, vol. 159, pp. 353–368, 2018.

[11] M. Errouha, A. Derouich, S. Motahhir, O. Zamzoum, N. El Ouanjli, and A. El Ghzizal, "Optimization and control of water pumping PV systems using fuzzy logic controller," *Energy Reports*, vol. 5, pp. 853–865, 2019.

[12] S. Rafa, A. Larabi, L. Barazane, M. Manceur, N. Essounbouli, and A. Hamzaoui, "Implementation of a new fuzzy vector control of induction motor," *ISA Transactions*, vol. 53, no. 3, pp. 744–754, 2014.

[13] M. Errouha, A. Derouich, B. Nahid-Mobarakeh, S. Motahhir, and A. El Ghzizal, "Improvement control of photovoltaic based water pumping system without energy storage," *Solar Energy*, vol. 190, pp. 319–328, 2019.

[14] I. M. Alsofyani and N. R. N. Idris, "A review on sensorless techniques for sustainable reliablity and efficient variable frequency drives of induction motors," *Renewable and Sustainable Energy Reviews*, vol. 24, pp. 111–121, 2013.

[15] N. El Ouanjli, A. Derouich, A. El Ghzizal et al., "Modern improvement techniques of direct torque control for induction motor drives-a review," *Protection and Control of Modern Power Systems*, vol. 4, no. 1, 2019.

[16] M. Errouha and A. Derouich, "Study and comparison results of the field oriented control for photovoltaic water pumping system applied on two cities in Morocco," *Bulletin of Electrical Engineering and Informatics*, vol. 8, no. 4, 2019.

[17] N. El Ouanjli, S. Motahhir, A. Derouich, A. El Ghzizal, A. Chebabhi, and M. Taoussi, "Improved DTC strategy of doubly fed induction motor using fuzzy logic controller," *Energy Reports*, vol. 5, pp. 271–279, 2019.

[18] D. Mohan, S. Member, X. Zhang, and G. Foo, "Generalized DTC strategy for multilevel inverter fed IPMSMs with constant inverter switching frequency and reduced torque ripples," *IEEE Transactions on Energy Conversion*, vol. 32, no. 3, pp. 1031–1041, 2017.

[19] D. Islam, C. M. F. S. Reza, and S. Mekhilef, "Modeling and experimental validation of 5-level hybrid H-bridge multilevel inverter fed DTC-IM drive," *Journal of Electrical Engineering and Technology*, vol. 10, no. 2, pp. 574–585, 2015.

[20] B. Singh, U. Sharma, and S. Kumar, "Standalone photovoltaic water pumping system using induction motor drive with reduced sensors," *IEEE Transactions on Industry Applications*, vol. 54, no. 4, pp. 3645–3655, 2018.

[21] S. Motahhir, A. El Hammoumi, and A. El Ghzizal, "The most used MPPT algorithms: review and the suitable low-cost embedded board for each algorithm," *Journal of Cleaner Production*, vol. 246, article 118983, 2020.

[22] A. Loukriz, M. Haddadi, and S. Messalti, "Simulation and experimental design of a new advanced variable step size incremental conductance MPPT algorithm for PV systems," *ISA Transactions*, vol. 62, pp. 30–38, 2016.

[23] S. Motahhir, A. El Ghzizal, S. Sebti, and A. Derouich, "Modeling of photovoltaic system with modified incremental conductance algorithm for fast changes of irradiance," *International Journal of Photoenergy*, vol. 2018, Article ID 3286479, 13 pages, 2018.

[24] C. M. F. S. Reza, M. D. Islam, and S. Mekhilef, "A review of reliable and energy efficient direct torque controlled induction motor drives," *Renewable and Sustainable Energy Reviews*, vol. 37, pp. 919–932, 2014.

[25] E. E. Aboul Zahab, A. M. Zaki, and M. M. El-sotouhy, "Design and control of a standalone PV water pumping system," *Journal of Electrical Systems and Information Technology*, vol. 4, no. 2, pp. 322–337, 2017.

[26] S.-H. Kim, "Brushless direct current motors," in *Electric Motor Control*, pp. 389–416, Science Direct, 2017.

[27] A. A. S. Mohamed, A. Berzoy, and O. Mohammed, "Optimized-fuzzy MPPT controller using GA for stand-alone photovoltaic water pumping system," in *ECON 2014 - 40th Annual Conference of the IEEE Industrial Electronics Society*, Dallas, TX, USA, 2014.

[28] R. Rai, S. Shukla, and B. Singh, "Sensorless field oriented ISMCC for solar PV based induction motor drive for water pumping," in *2019 IEEE International Conference on Environment and Electrical Engineering and 2019 IEEE Industrial and Commercial Power Systems Europe (EEEIC / I&CPS Europe)*, Genova, Italy, 2019.

[29] Z. Salam, J. Ahmed, and B. S. Merugu, "The application of soft computing methods for MPPT of PV system: a technological and status review," *Applied Energy*, vol. 107, pp. 135–148, 2013.

[30] M. A. Hannan, J. A. Ali, A. Mohamed, and A. Hussain, "Optimization techniques to enhance the performance of induction motor drives: a review," *Renewable and Sustainable Energy Reviews*, vol. 81, pp. 1611–1626, 2018.

[31] S. Gdaim, A. Mtibaa, and M. F. Mimouni, "Design and experimental implementation of DTC of an induction machine based on fuzzy logic control on FPGA," *IEEE Transactions on Fuzzy Systems*, vol. 23, no. 3, pp. 644–655, 2015.

[32] H. Sudheer, S. F. Kodad, and B. Sarvesh, "Improvements in direct torque control of induction motor for wide range of speed operation using fuzzy logic," *Journal of Electrical Systems and Information Technology*, vol. 5, no. 3, pp. 813–828, 2018.

[33] S. Motahhir, A. Chouder, A. El Hammoumi et al., "Optimal energy harvesting from a multistrings PV generator based on artificial bee colony algorithm," *IEEE Systems Journal*, pp. 1–8, 2020.

[34] L. Shang, W. Zhu, P. Li, and H. Guo, "Maximum power point tracking of PV system under partial shading conditions through flower pollination algorithm," *Protection and Control of Modern Power Systems*, vol. 3, no. 1, 2018.

[35] S. Salman, X. Ai, and Z. Wu, "Design of a P-&-O algorithm based MPPT charge controller for a stand-alone 200W PV system," *Protection and Control of Modern Power Systems*, vol. 3, no. 1, 2018.

[36] N. El Ouanjli, A. Derouich, A. El Ghzizal, Y. El Mourabit, B. Bossoufi, and M. Taoussi, "Contribution to the improvement of the performances of doubly Fed induction machine functioning in motor mode by the DTC control," *International Journal of Power Electronics and Drive Systems (IJPEDS)*, vol. 8, no. 3, pp. 1117–1127, 2017.

[37] C. N. Bhende and S. G. Malla, "Novel control of photovoltaic based water pumping system without energy storage," *International Journal of Emerging Electric Power Systems*, vol. 13, no. 5, 2012.

[38] A. El Hammoumi, S. Motahhir, A. Chalh, A. El Ghzizal, and A. Derouich, "Real-time virtual instrumentation of Arduino and LabVIEW based PV panel characteristics," *IOP Conference Series: Earth and Environmental Science*, vol. 161, no. 1, article 012019, 2018.

[39] I. Yahyaoui, M. Chaabene, and F. Tadeo, "Evaluation of maximum power point tracking algorithm for off-grid photovoltaic pumping," *Sustainable Cities and Society*, vol. 25, pp. 65–73, 2016.

[40] M. Errouha, S. Motahhir, Q. Combe, A. Derouich, and A. El Ghzizal, "Fuzzy-PI Controller for Photovoltaic Water Pumping Systems," in *2019 7th International Renewable and Sustainable Energy Conference (IRSEC)*, Agadir, Morocco, Morocco, 2019.